atmosphere

MDPI

Article

Variation Characteristics of Pavement Temperature in Winter and Its Nowcasting for Xianyang Airport Expressway, China

Lei Feng [1,2], Hua Tian [1,2,*], Xiaoyu Yuan [1,*], Lei Miao [1] and Mingyu Lin [1]

[1] Public Meteorological Service Center of China Meteorological Administration, Beijing 100081, China
[2] Key Laboratory of Transportation Meteorology of China Meteorological Administration, Nanjing Joint Institute for Atmospheric Sciences, Nanjing 210041, China
* Correspondence: tianh1@cma.gov.cn (H.T.); yuanxy@cma.gov.cn (X.Y.)

Abstract: Based on the pavement temperature observation data of the transportation meteorological stations along the Xianyang Airport Expressway, China, as well as the datasets of precipitation and sunshine hours obtained from the nearby weather stations, the variation characteristics of local pavement temperatures are investigated for winter in this study. Results indicate that during the daytime, the pavement temperatures are always higher on sunny and cloudy days than those on rainy and snowy days, while during the nighttime, the temperatures on sunny and cloudy days are higher than those on the days with freezing rain and snow, and with the temperatures on rainy and snowy days without icing being further higher. In general, the pavement temperatures in winter features significant periodic oscillations with cycles of roughly 24 h, 12 h, 8 h, 6 h, 5 h and 4 h, which differ slightly at different times for different stations. Moreover, the nowcasting experiments on the local pavement temperatures are also carried out using a regression model via extracting the corresponding periodic features. It shows the mean absolute errors of about 0.6 °C, 1.2 °C, and 1.5 °C for lead times of 1 h, 2 h, and 3 h, respectively. The nowcasting skills are higher on rainy and snowy days, while are inferior on sunny days. For nowcasting cases initialized at nighttime (daytime), the mean absolute errors are 0.4 °C (0.7 °C) and 0.9 °C (1.4 °C) for lead times of 1 h and 2 h. Examinations suggest that the nowcasting system could be well utilized in plain areas of China, whereas it shows relatively larger biases in plateau areas with complex terrain.

Keywords: pavement temperature; nowcasting; variation characteristics; forecast validation

Citation: Feng, L.; Tian, H.; Yuan, X.; Miao, L.; Lin, M. Variation Characteristics of Pavement Temperature in Winter and Its Nowcasting for Xianyang Airport Expressway, China. *Atmosphere* **2023**, *14*, 361. https://doi.org/10.3390/atmos14020361

Academic Editor: Graziano Coppa

Received: 13 January 2023
Revised: 28 January 2023
Accepted: 8 February 2023
Published: 11 February 2023

1. Introduction

In winter, the low temperature combined with the rain and snow tend to trigger freezing events and lead the road to be slippery. It increases the braking distance and reduces the anti-sideslip ability of vehicles, which poses severe threats to transportation safety. Previous statistics have revealed that the collision and scraping accidents of vehicles in snowy weathers are roughly 14 times of those in sunny weathers [1]. In China, the traffic accidents in snowy days account for 6.93% of the total, thus being the second most crucial meteorological factor for inducing traffic accidents. On 7 December 2001, slight snowfall in Beijing caused a severe traffic jam in the city due to its coincidence with the off-duty traffic peak [2,3].

The pavement temperature forecast is one of the most important parameters for predicting road icing and snow. It directly affects the effectiveness of road icing and snow state identification in the near future. The current study focuses on the Xi'an Xianyang Airport Expressway in China, which is the traffic artery leading to the airport in Xi'an with large traffic flows. However, its safe and smooth operation is certainly threatened by weathers of low temperature, rain, snow and freezing. Therefore, it is of great significance to investigate the temporal variation characteristics of local pavement temperature in winter and its nowcasting, which is favorable for effective forecasts of snow and icing on the

airport expressway. At the same time, the nowcasting method established for this region is helpful to improve the pavement temperature prediction for other areas [4].

With respect to the prediction techniques of pavement temperatures, the physical models have already been developed based on the surface energy balance earlier in the United States and several countries in Europe [5–9]. Additionally, these models have also been continuously improved and optimized by revealing the interactions between meteorological and pavement conditions [10,11]. Generally, the mechanisms of pavement temperature predictions have been studied well, and multiple numerical models have been used worldwide [12]. Meanwhile, on this basis, combined with the multi-source data fusion analysis and forecasting system, several methods have been developed on refined predictions of pavement temperatures, which could be scrolled at high frequencies and could better meet the requirements of transportation users [13,14].

In China, investigations on pavement transportation meteorology started relatively late. In recent decades, some provinces such as Jiangsu, Beijing and Hebei have organized transportation meteorological operational businesses to deal with the severe effects of low temperature, rainy, snowy and freezing weathers on pavement traffic [15–17]. Multiple physical and statistical models have been established to automatically predict the pavement temperatures, which are examined and demonstrated to be effective in local forecast businesses [18]. These models are generally combined with the applications of numerical prediction products and the lead times mainly range from 0 to 24–48 h [19,20]. It is of great significance for the identification of low temperature, rainy, snowy and freezing events in the short term [21,22]. The predictions of pavement conditions are affected by plenty of factors including not only the accuracy of meteorological forecasts but also the initial observation of transportation road surfaces, the shading effect of surrounding obstructions, the emission of human activities, and the pavement heat conductions, etc. Therefore, the forecast accuracy of pavement conditions such as temperatures is generally limited and less skillful than that of the conventional meteorological elements [23,24].

The accurate perception and prediction of pavement status play crucial roles in the realization of vehicle–road coordination and establishment of the smart highway. The refined meteorological services on hundred-meter-level and minute-level resolutions are becoming an important guarantee for smart transportation capacities at all weather conditions. In recent years, the departments of public security, transportation and meteorology have cooperated on the joint prevention and mitigation of severe weather impacts, which brings about the increasing demands for forecasts of low temperature and icing pavements with higher resolution and accuracy. In general, the forecast skills tend to decrease (increase) with longer (shorter) lead times. Tang and Guo [25] used the autoregressive summation moving average method to explore the fluctuation pattern of winter pavement temperature in the near future under the impacts of external factors, and constructed a short-term forecast model of winter pavement temperature with lead times of 3 h based on the transportation meteorological observations at minute-by-minute intervals. Further, Wang et al. [26] carried out the nowcasting experiments using the random forest regression method for transportation meteorological stations alongside the Ning-Su-Xu Expressway in Jiangsu Province, detecting the influences of different input schemes and parameters of different observation stations on the pavement temperature forecasts. On the basis of the physical METRo model with surface energy balance principles, Qu et al. [27] conducted studies on the 0–6 h forecasts of pavement temperatures for the Beijing–Zhangjiakou Olympic Winter Games-associated expressway, revealing that the forecast during nighttime is characterized by root-mean-square errors of ~1 °C and is superior to that during daytime. Comparisons indicate that the statistical methods constructed on the observation analyses show generally higher forecast skills than the physical models based on the surface energy balance for the nowcasting of pavement temperatures [25–27].

In the current paper, the variation characteristics of observed pavement temperature in winter are to be investigated for two transportation meteorological stations along the Xianyang Airport Expressway in Xi'an, China. On this basis, a pavement temperature

nowcasting method is proposed via extracting the periodic features of the temperature temporal series and constructing the associated regression model, which is examined for pavement temperature nowcasting experiments at a 10 min rolling update and a 10 min interval. Meanwhile, the impacts of different sample amounts, different weather conditions, and different initialization times on the nowcasting effects are also investigated in detail. In addition, similar examinations on pavement temperature nowcasting are carried out for multiple expressways to further verify the applicability of the proposed method for different regions.

2. Dataset and Methodology

2.1. Dataset

The hourly observation datasets of the two transportation meteorological stations (V0001 (108.92° E, 34.37° N) and V0002 (108.90° E, 34.43° N), as shown in Figure 1) along the Xianyang Airport Expressway in Xi'an, China were obtained for the two winters of 2018/2019 and 2019/2020 from the data platform of China Meteorological Administration. The two stations are located at the two ends of the No. 2 Grand Bridge over the Weihe River. Station V0001 is in the suburban area. There are many building facilities around, and the traffic flow is relatively complex. Station V0002 is located in the outer suburbs. It is surrounded mainly by farmland, and there are also a few buildings. The altitudes of Stations V0001 and V0002 are 37.1 m and 40.7 m, respectively. The observation elements include pavement temperature, surface air temperature, wind speed, wind direction and relative humidity. The pavement temperature was measured by using embedded thermal sensor with platinum rod-shaped probe. It was noted that most transportation meteorological stations have not yet been equipped with weighing precipitation sensors due to the maintenance difficulties and the solid precipitation such as snowfall could hardly be monitored. Therefore, the hourly precipitations over the two transportation meteorological stations were approximately substituted by the observations of the neighboring national weather station (Station 57131), which is 10.1 km and 7.3 km far from Stations V0001 and V0002, respectively. In addition, comprehensive observations such as sunshine hours from Station 57131 were also employed to determine weather conditions (sunny, cloudy, rainy, and snowy, etc.) at the transportation meteorological stations. Based on these hourly observation datasets, the basic characteristics of pavement temperature variations on the expressways were analyzed for the wintertime.

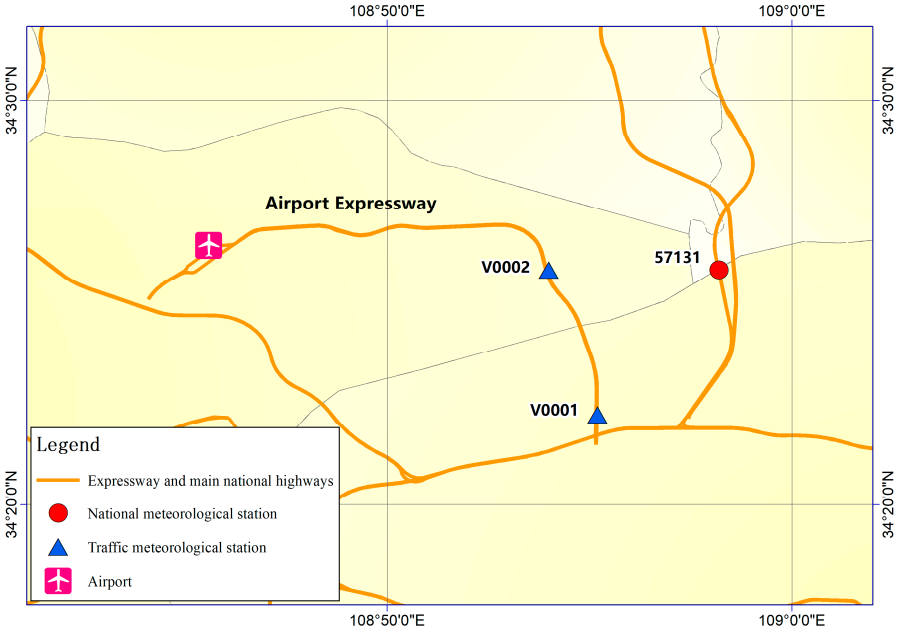

Figure 1. Locations of the transportation meteorological stations along Xianyang Airport Expressway in Xi'an, China, and the neighboring national meteorological station.

In order to verify the rationality of taking the national station observation (e.g., precipitation, sunshine hours, etc.) as substitutions for the two transportation meteorological stations, Table 1 shows the statistics of observed temperature and wind among the three stations for the total of 181 days in the two winters of 2018/2019 and 2019/2020. It is indicated that the temperatures at Station V0001 (V0002) are slightly higher (lower) than those at Station 57131, with their differences in daily mean, maximum and minimum temperatures being 0.65 °C (1.19 °C), 0.76 °C (1.03 °C) and 0.58 °C (1.35 °C), respectively. Such spatial differences might be associated with the urban heat island effects and the local environment of these stations. Besides, the correlation coefficients between the daily mean temperature series of the two transportation meteorological stations and the national observation station are both greater than 0.97, with that of Station V0001 being higher than V0002 and reaching up to 0.99. As for the wind speed, the daily averages and maximums at the two transportation meteorological stations are all lower than those at the national observation station. The daily average and maximum wind speeds at Station V0001 (V0002) are characterized by values of 0.77 m/s (1.13 m/s) and 1.00 m/s (1.41 m/s) lower than those of Station 57131, respectively, and show correlation coefficients of 0.95 (0.80) and 0.95 (0.68) with the observations from the national station. The comparison analyses demonstrate that the meteorological conditions at the two transportation meteorological stations are generally similar to those of the neighboring national meteorological station. Therefore, the observations of precipitation and sunshine hours at Station 57131 could be reasonably taken as the corresponding status of the two transportation meteorological stations.

Table 1. Statistics of observed temperature and wind speed for Station 57131 and Stations V0001 and V0002 in the two winters, including the respective temporal averages (TAs, units: °C for temperature and m/s for wind speed) and the correlation coefficients (CCs) of the two transportation meteorological stations V0001 and V0002 to the national station 57131.

Station ID	Daily Average Temperature		Daily Maximum Temperature		Daily Minimum Temperature		Daily Average Wind Speed		Daily Maximum Wind Speed	
	TA	CC	TA	CC	TA	CC	TA	CC	TA	CC
57131	3.22	-	3.61	-	2.83	-	2.05	-	2.62	-
V0001	3.87	0.99	4.37	0.99	3.41	0.99	1.28	0.95	1.62	0.95
V0002	2.03	0.98	2.58	0.98	1.48	0.97	0.92	0.80	1.21	0.68

Observations with high frequency and high accuracy are the most basic fundamentals to carry out effective early warnings and predictions of pavement low temperature and road icing. In this study, the pavement temperature observations at the two transportation meteorological stations were obtained every 10 min during the winter in 2018/2019 (90 days in total, composing 12,960 samples for each station) for investigations of pavement temperature nowcasting. In general, they had relatively complete datasets, except the period of 7:00 to 13:00 on 30 December 2018 and several other missing observations, which were further supplemented with linear interpolations. Calculations on the observations show that the mean pavement temperature and the corresponding mean square deviation are 3.31 °C (3.17 °C) and 4.54 °C (3.73 °C) for Station V0001 (V0002), respectively. Significant differences (at the 95% confidence level according to the Student's *t*-test) are observed between the two stations.

Based on the nowcasting experiments on pavement temperatures for the two transportation meteorological stations along the Xianyang Airport Expressway, the proposed method was further promoted and examined towards three stations in three different-climate regions (Beijing, Hubei and Tibet). The method applicability was verified for the three different places via pavement temperature nowcasting experiments at a 10 min rolling update and a 10 min interval for the winter of 2021/2022. The geographical information of the three transportation meteorological stations is displayed in Table 2.

Table 2. Geographical information of the three transportation meteorological stations in Beijing, Hubei and Tibet, respectively.

Station ID	Region	Expressway	Longitude	Latitude	Altitude
A1412	Changping, Beijing	West Sixth Ring Road (G4501)	116.11° E	40.13° N	75 m
Q0007	Enshi, Hubei	Shanghai-Chongqing Expressway (G50)	109.37° E	30.24° N	708 m
U1801	Lhasa, Tibet	Ya'an–Yecheng Expressway (G4218)	90.95° E	29.45° N	3610 m

2.2. Methodology

2.2.1. Classification of Weather Types

Using the precipitation and sunshine hour observations from Station 57131, the weather conditions were classified into several categories, which represented the weather of the two transportation meteorological stations along the airport expressway. The variation characteristics and nowcasting skills of pavement temperatures were subsequently analyzed towards different weather conditions. Following Wu et al. [28] and Ma et al. [29], the days with sunshine hours of ≥3 h and no precipitation were defined as sunny days, while those with sunshine hours of <3 h and no precipitation were defined as cloudy days, and the others are rainy and snowy days. It is noted that the observations of pavement conditions were not included in the transportation meteorological stations. Therefore, the pavement icing on rainy and snowy days needed to be recognized via the associated elements, e.g., the simultaneous conditions of low pavement temperature (≤0 °C) and precipitation occurrence at the neighboring national meteorological station [30], which have been examined and demonstrated to be effective in previous studies on transportation meteorological information at Lianyungang–Khorgos Expressway (G30) [31].

2.2.2. Nowcasting of Pavement Temperature

In this paper, the nowcasting of pavement temperature was constructed via the extraction of periodic features of local pavement temperature series and the subsequent regression procedures. Firstly, the power spectrum was employed to analyze the periodic oscillation characteristics of the local pavement temperature series. It is a frequency domain analysis method based on Fourier transform, which decomposes the total energy of the time series into components at different frequencies, and diagnoses the main cycle of the series according to the corresponding variance contributions, so as to determine the implied main frequency and cycles of the series [32,33]. The calculation formula of power spectrum intensity is as follows:

$$\hat{s_k} = \frac{1}{m}\left[r(0) + 2\sum_{j=1}^{m-1} r(j)cos\frac{k\pi j}{m} + r(m)cosk\pi\right],\ k = 0, 1, \ldots, m \tag{1}$$

$$r(j) = \frac{1}{n-j}\sum_{t=1}^{n-j}\left(\frac{x_t - \bar{x}}{s}\right)\left(\frac{x_{t+j} - \bar{x}}{s}\right) \tag{2}$$

where k is the wave number, $\bar{x}$ is the mean value of the sequence, s is the standard deviation of the sequence, and m is the maximum lag time length. The value of m is generally taken as $n/3$, where n is the sample.

On this basis, the red noise power spectrum test was utilized to examine the significance of the obtained periodic characteristics. The calculation formula of the red noise standard spectrum is as follows:

$$s_{0k} = \bar{s}\left[\frac{1 - r(1)^2}{1 + r(1)^2 + 2r(1)cos\frac{\pi k}{m}}\right],\ k = 0, 1, \ldots, m \tag{3}$$

$$\bar{s} = \frac{1}{2m}(s_0 + s_m) + \frac{1}{m}\sum_{k=1}^{m-1} s_k,\ k = 0, 1, \ldots, m \quad (4)$$

The power spectra ratio is defined as $\hat{s_k}/s_{0k}$ to detect the significant period. The significant periodic functions of the pavement temperature time series were then extracted using the mean-generation function model.

The mean-generation function was derived from the mean values at certain time intervals of the time series. The domain of the function definition was extended to the entire axis, which is called the periodic extension. The mean-generation function model could be well used in multi-step forecasts as well as extreme predictions and has been widely exploited in long-term weather forecasts and short-term climate predictions [34,35].

The sequence stationarity is one of the important prerequisites for analysis and modeling of the temporal series, while previous studies have revealed the significant non-stationary characteristics of the pavement temperature [25]. Therefore, the first-order difference method was used in this study to make the original sequence of pavement temperatures stabilized, in which the differential sequence of pavement temperature was taken as the dependent variable and all periodic function sequences passing the confidence level were used as the independent variables. The nowcasting model of pavement temperature can be constructed by the multiple linear regression method with the significant periodic function extended to the entire axis. The inversed differential calculation was, hence, carried out to obtain the forecast results of pavement temperatures for the next 6 h by every 10 min. Similar methods have achieved considerable effects in wind-nowcasting experiments [36].

For the two transportation meteorological observation stations V0001 and V0002, the pavement temperatures of every 10 min during the past 3 days before the current moment were used as the training dataset to predict the pavement temperatures at intervals of 10 min in the next 6 h. The forecast framework was updated with real-time observations with a rolling frequency of 10 min. Taking the first forecast experiment in this study (initialized at 23:00 3 December 2018) as an example, the pavement temperature series during 00:00 1 December to 23:00 3 December by every 10 min were firstly preprocessed by the first-order difference. Afterwards, the periodic functions passing the significance test were extracted through procedures of the power spectrum analysis, the red noise test, and the mean-generation function to construct the nowcasting model of the pavement temperature. The pavement temperature forecasts for the next 6 h at 10 min intervals since 00:00 4 December 2018 were then obtained based on the extended series of periodic functions and the inversed differential calculation.

Moreover, the same framework of nowcasting was also carried out and examined towards Station V0002 in Shanxi and the three transportation meteorological stations in Beijing, Hubei and Tibet using the 10-by-10 min observations in the winter of 2021/2022 to further investigate the applicability of the nowcasting method in multiple areas.

3. Results

3.1. Characteristics of Pavement Temperature Variations

3.1.1. Diurnal Variation Characteristics

In the two winters of 2018/2019 and 2019/2020 except the day with serious data deficiency (30 December 2018), there were 88 sunny days and 78 cloudy days. As for the rainy and snowy days, there were 2 (1) days with and 12 (13) days without icing at Station V0001 (V0002). Figure 2 shows the diurnal variations of pavement temperature on sunny days, cloudy days and rainy and snowy days (with unfrozen and frozen road surfaces). Under the multiple weather conditions, the pavement temperature is characterized by significant diurnal variations, showing the highest values in the early afternoon and lowest at around 07:00–08:00 in the morning. Furthermore, the sunny (rainy and snowy) days are featured by the highest (smallest) diurnal ranges of pavement temperature, and those in the cloudy days are located in between. The pavement temperature on sunny days is generally higher than cloudy and rainy and snowy days in the daytime. However, it decreases rapidly

and becomes lower than that on cloudy and rainy and snowy days without icing in the nighttime and early morning but still higher than that on rainy and snowy days with icing. This is due to that the clouds on cloudy and non-icing rainy and snowy days tend to block the solar shortwave radiation reaching the surface, leading to relatively lower pavement temperatures in the daytime, while in the nighttime, they suppress the longwave radiation releasing out of the atmosphere from the surface, which induces the higher pavement temperatures than the sunny days with clear sky. On the other hand, the rainy and snowy days with icing show obviously lower pavement temperatures than the other conditions in both daytime and nighttime, which could be attributed to the joint impacts from the systematic cooling processes of the atmosphere and the reflection of solar radiation by snow or ice on the pavement surface. It may also be related to the definition of weather type in Section 2.2.1.

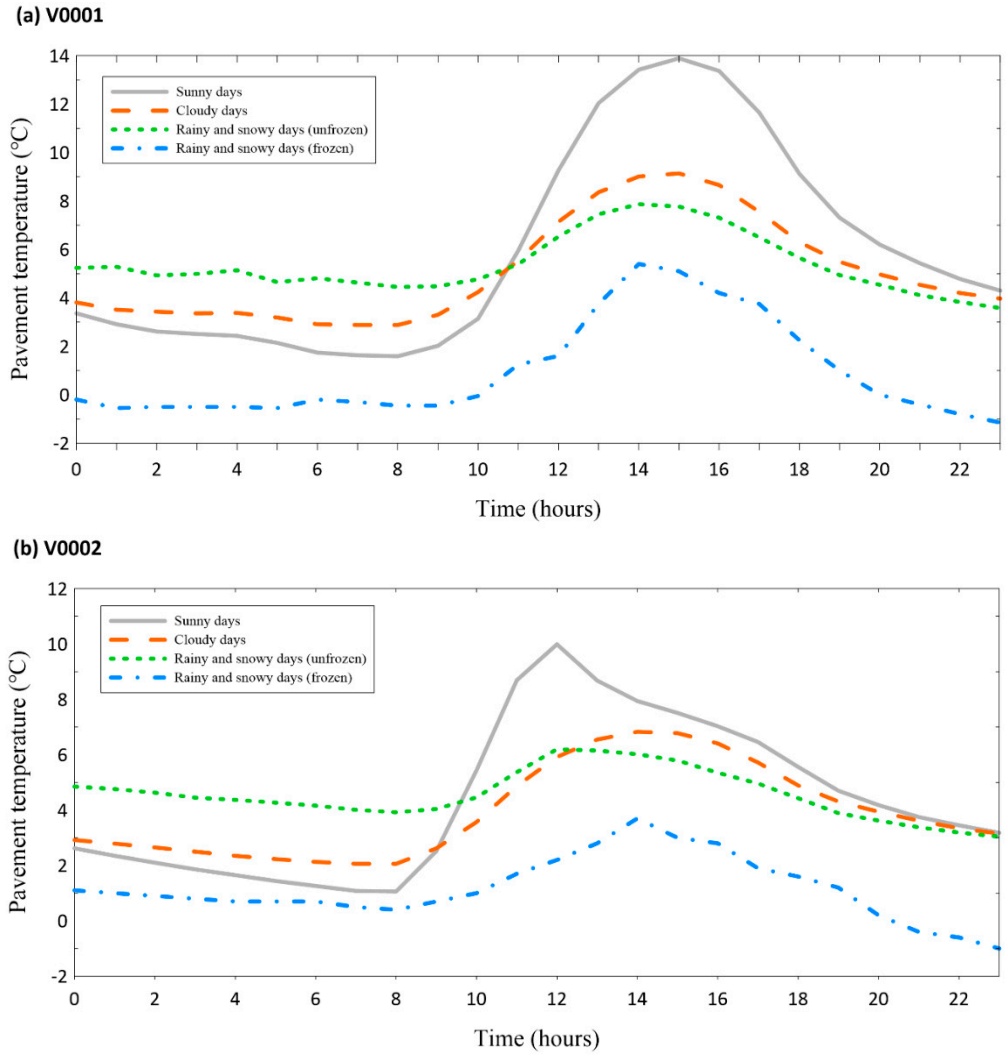

Figure 2. Diurnal variations of pavement temperatures at Stations V0001 (**a**) and V0002 (**b**) under different weather conditions.

Table 3 further displays the temporal averages and mean square deviations of pavement temperatures in the daytime and nighttime at Stations V0001 and V0002 under different weather conditions. According to the local characteristics of sunrise and sunset in winter, the daytime and nighttime are determined as 08:00–18:00 and 19:00–07:00 of the next day, respectively. It verifies the highest pavement temperatures in the daytime of sunny days among the several cases, which is meanwhile accompanied with the largest variability in temperature. In the nighttime, the pavement temperature is highest in non-

icing rainy and snowy cases, and is the lowest (maintaining at around 0 °C) in icing rainy and snowy ones with the corresponding variability also being the smallest. Additionally, in the daytime, the pavement temperatures in the sunny days are significantly different from those under the other weather conditions passing the Student's *t*-test at the 95% confidence level, while the pavement temperatures in cloudy days and rainy and snowy days do not differ significantly. As for the nighttime, the differences in pavement temperatures among these several weather conditions are all non-significant according to the Student's *t*-test.

Table 3. Temporal averages (AVE; units: °C) and mean square deviations (MSD; units: °C) of pavement temperatures in the daytime and nighttime at Stations V0001 and V0002 under different weather conditions.

Weather Condition	V0001				V0002			
	Daytime		Nighttime		Daytime		Nighttime	
	AVE	MSD	AVE	MSD	AVE	MSD	AVE	MSD
Sunny	8.68	4.84	3.64	1.98	6.44	2.81	2.59	1.28
Cloudy	6.55	2.39	3.82	1.15	5.11	1.76	2.92	0.91
Rainy and snowy (unfrozen)	6.20	1.51	4.67	1.04	5.15	1.11	4.05	0.82
Rainy and snowy (frozen)	2.40	2.20	−0.36	0.61	1.98	1.04	0.45	0.69

3.1.2. Power Spectrum Features

In order to investigate the detailed periodic features of pavement temperature variations, the power spectrum analysis (Figure 3) was carried out towards the 12,960 data samples which consisted of the pavement temperature observations by every 10 min in the winter of 2018/2019 for Stations V0001 and V0002, respectively. The horizontal axis denotes the length of cycle period, and the vertical axis is the power spectral density of the corresponding cycle divided by the red noise standard spectrum at $\alpha = 0.05$ as described in Section 2.2.2. The spectral ratio of >1.0 represents the periodic significance at the 95% confidence level. The greater the ratio, the more significant the cycle.

As shown in Figure 3, the power spectra of pavement temperatures at the two stations display several significant peaks, locating at the cycle lengths of roughly 24 h, 12 h, 8 h, 6 h, 5 h and 4 h, which are all characterized by power spectrum ratios of >1.0. The first two leading cycles reflect the diurnal and semi-diurnal variations of pavement temperature, which are similar to the variations of surface air temperature and have been well revealed by previous studies. The obvious periodic pattern shows a single peak at noon and a single valley in the early morning [37]. However, the pavement temperatures are also characterized by significant intra-diurnal high-frequency periodic oscillations with periodic cycles of 8 h, 6 h, 5 h and 4 h, which have been seldom mentioned.

The change in the pavement temperature is affected by many factors, such as solar radiation, cloud cover, air temperature, wind speed, relative humidity, pressure, etc. Power spectrum analysis has been conducted for temperature, wind speed and humidity variables, and it was found that these variables also have significant short-period oscillation, especially for temperature and humidity. Studies on periodic variation of wind speed based on Morlet wavelet transformation indicates that on the daily time scale, the wind speed has a significant period of 8 h, 12 h and 24 h [38]. Smaller scale oscillations of the pavement temperature may be related with the short-period variation of other weather variables or the interaction of multiple variables. More comprehensive observation data are needed for a deeper analysis of this problem.

In order to study the intra-diurnal variations of pavement temperatures in more detail, taking the period from 1 December 2018 to 28 February 2019 as an example, power spectrum analysis is performed on the daily pavement temperature series by every 10 min (composing 144 samples in total). With reference to the intraseasonal oscillation analysis on the persistent heavy rainfall in Southern China by Wei et al. [35], the daily power spectral

density is divided by the red noise standard spectrum at $\alpha = 0.05$, which are plotted as the distributions of daily power spectrum ratios of pavement temperatures (Figure 4).

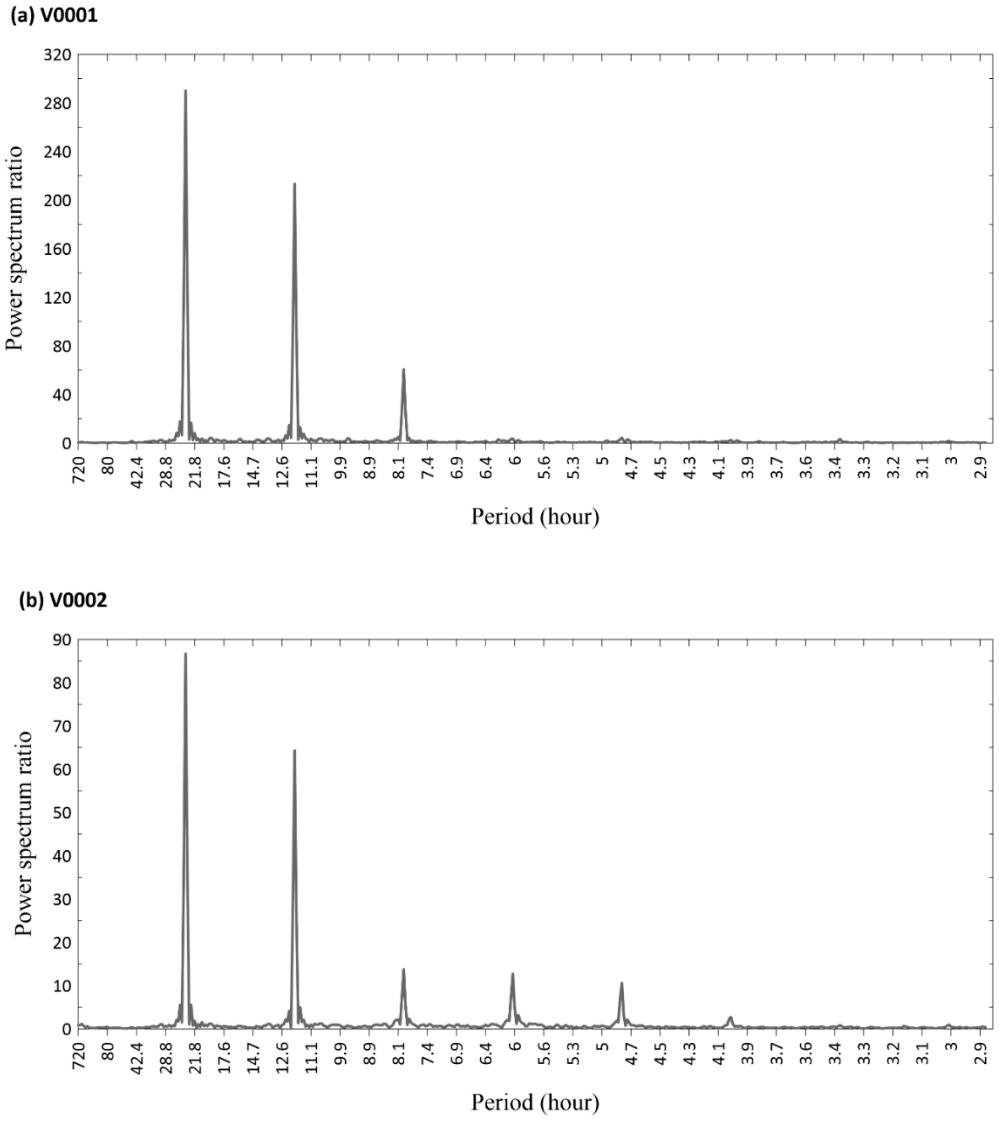

Figure 3. Power spectrum ratios of pavement temperatures by every 10 min in the winter of 2018/2019 for Stations V0001 (**a**) and V0002 (**b**).

It is indicated that there are both significant periodic oscillations with cycles of 6–12 h in the pavement temperature variations of the two transportation meteorological stations. The distribution of power spectrum ratios suggests that certain but limited differences exist in the periodic characteristics of pavement temperatures between the two stations and among different days. The significant periodic oscillations of 6–12 h are relatively stable throughout the winter. Among them, during the periods of 45th–46th days (14–15 January 2019), the 59th–60th days (28–29 January 2019), and the 70th day (8 February 2019), the periodic characteristics of pavement temperatures are generally weaker than those during other periods. The weather conditions are checked to be mainly cloudy during the above periods. In addition, the two pavement temperature series are also featured with periodic oscillations of 4–5 h, with more significant characteristics in Station V0002 than Station V0001 from the perspective of the power spectrum ratio. That is, although the two stations are located in the same climate region, obvious differences might occur between their periodic characteristics of pavement temperatures due to their differences in local environments. Therefore, it is of great importance to grasp the precise periodic

features based on the observations of the station, which play a crucial role in the accurate predictions of local pavement temperature.

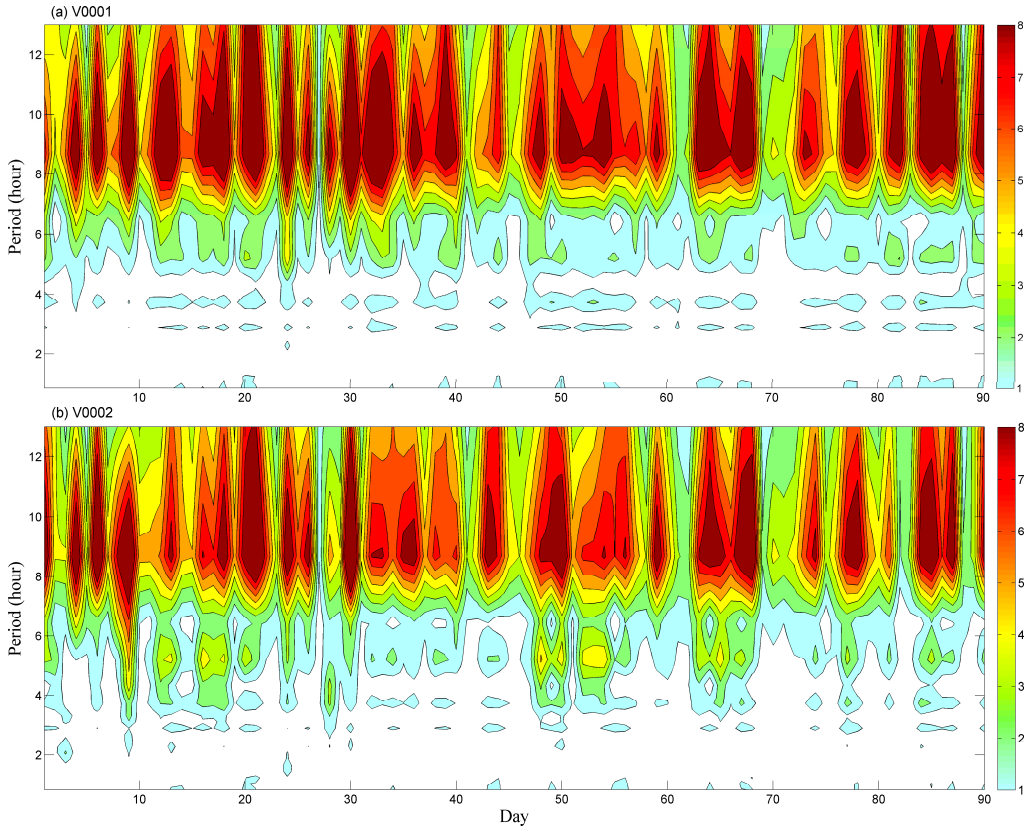

Figure 4. Distribution of daily power spectrum ratios of pavement temperatures in the winter of 2018/2019 for Stations V0001 (**a**) and V0002 (**b**). The shading denotes the significance at the 95% confidence level.

3.2. Nowcasting of Pavement Temperatures and the Validation

3.2.1. Impacts from Sample Sizes on Forecast Results

In this study, the nowcasting model is constructed based on the oscillation analysis of the pavement temperature series over certain periods in the past. Theoretically, it could describe more details of the pavement temperature variations with more observation samples used and provide more accurate predictions. However, the larger sample size would definitely result in greater computational complexity. Meanwhile, such a nowcasting model consisting of observations has high requirements for data quality and integrity. Due to the lack of maintenance with standardized processes, the transportation meteorological stations generally lack in quality compared with the normal meteorological observation stations, with the missing or abnormal data occurring more frequently. The data measures of quality control and numerical interpolation are necessary to improve the data application. Therefore, the workload of data preprocessing would also increase in correspondence with the larger sample size. In order to examine the impacts from sample sizes on the pavement temperature nowcasting, we used the 10-by-10 min observations of the first 3 days (432 samples), 4 days (576 samples), and 5 days (720 samples) for model constructions, respectively, with their forecast errors displayed and compared in Figure 5.

It can be seen that, for the two transportation meteorological stations, the increase in the sample sizes does not have obvious influences on the pavement temperature forecasts in the first 2 h. At Station V0001, the increasing sample sizes bring about only slight improvements on the forecasts in the first hour. After that, the forecast error even increases with more samples included, showing greater rising magnitudes at longer lead times. As for Station V0002, the forecast shows slightly higher skills in the first 4 h with the increase in

sample numbers, while the effect of sample sizes becomes unstable at lead times longer than that, playing positive roles with 576 samples but negative roles with 720 samples. Overall, the optimal sample size is determined as 432 (i.e., 3 days before the forecast initialization moment) in the subsequent nowcasting experiments.

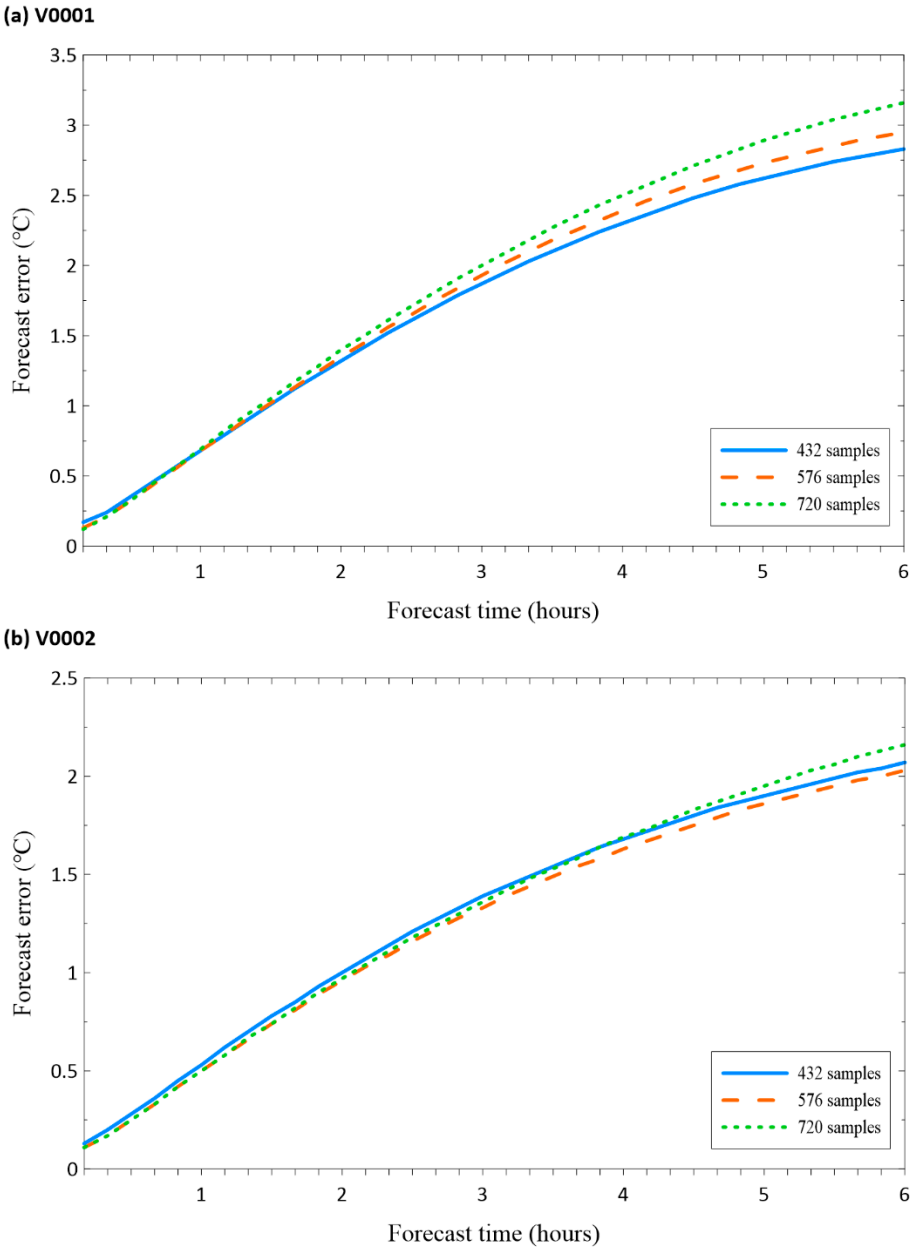

Figure 5. Impacts from sample sizes on forecast results of pavement temperatures for Stations V0001 (**a**) and V0002 (**b**).

3.2.2. General Evaluations of the Forecasts

Based on the methodology introduced in Section 2.2.2, rolling experiments of pavement temperature nowcasting were carried out for 23:00 on 3 December 2018 to 23:00 on 27 February 2019 using the pavement temperature observations in the previous 3 days. A total of 12,384 nowcasting experiment samples were obtained. Figure 6 displays the overall evaluations of pavement temperature nowcasting experiments for Stations V0001 and V0002 within lead times of 6 h by every 10 min. Forecasts for the two stations both show considerable skills within lead times of first few hours, while the forecast skills decrease significantly with the increasing lead time. The absolute errors of forecasts for

Stations V0001 and V0002 are no greater than 1 °C within lead times of 90 min and 120 min, respectively. Additionally, they show errors of <2 °C until lead times of 200 min and 330 min.

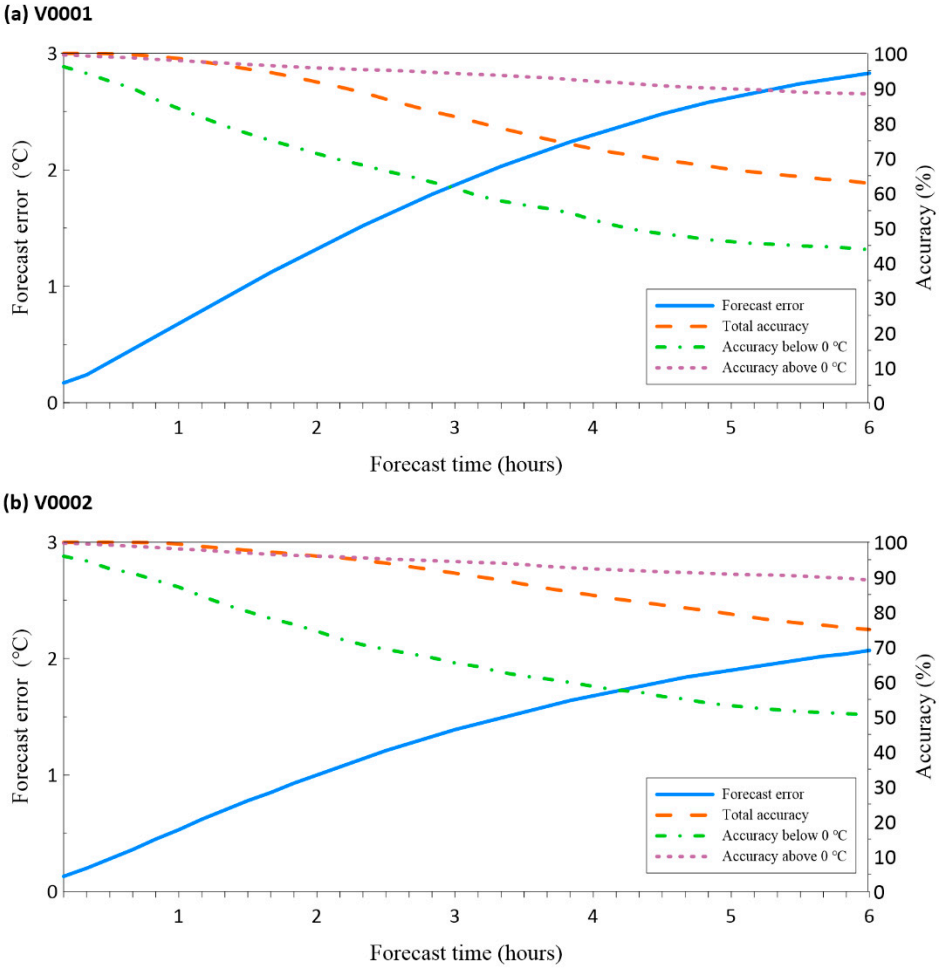

Figure 6. Evaluations of the pavement temperature nowcasting experiments by forecast errors (units: °C) and accuracies (units: %) for Stations V0001 (**a**) and V0002 (**b**), respectively.

Moreover, the statistics of ratios between the mean square deviations of the forecast errors at different lead times and those of the observed pavement temperature series are provided in Table 4. It is normally considered that the forecasts have practical application values with the ratio of <0.5. Forecasts for the two stations show similar skills with the ratios being no greater than 0.14, 0.26 and 0.36 for lead times of shorter than 1 h, 2 h and 3 h, respectively. It is implied that the proposed method could be well utilized in the nowcasting of pavement temperatures along the expressway.

Table 4. Ratios between the mean square deviations of the forecast errors at different lead times and those of the observed pavement temperature series.

Station	Lead Times (Units: 10 min)																	
	1	**2**	**3**	**4**	**5**	**6**	**7**	**8**	**9**	**10**	**11**	**12**	**13**	**14**	**15**	**16**	**17**	**18**
V0001	0.04	0.05	0.08	0.10	0.12	0.14	0.17	0.19	0.21	0.23	0.25	0.26	0.28	0.30	0.31	0.33	0.35	0.36
V0002	0.04	0.05	0.07	0.10	0.12	0.14	0.16	0.19	0.21	0.22	0.24	0.26	0.28	0.29	0.30	0.32	0.33	0.34

As for the forecast accuracy, when the pavement temperature observation and forecast are both positive (>0 °C) or both negative (<0 °C), it is considered a success, otherwise it is recorded as a failure. In general, the forecast accuracy rate for pavement temperatures

above 0 °C reaches 90% at even lead times of 360 min, which is much higher than that below 0 °C. Although the two stations both show accuracy rates greater than 85% for negative pavement temperatures within lead times of the first hour, it decreases rapidly from 96% to 50% from lead times of 10 min to 360 min. It may be related to the small number of cases with temperatures below 0 °C. For the climate of the area where Xianyang Airport is located, the condition of temperature below 0 °C is very rare. This may affect the prediction accuracy of the statistical model based on the variation characteristics of observation data.

In terms of the previous studies on pavement temperature nowcasting, Wang et al. [26] used the random forest regression method to predict pavement temperatures in the next one hour at three transportation meteorological stations along the Ning-Su-Xu Expressway in Jiangsu province, with the obtained nowcasting results showing mean absolute errors of 0.92 °C, 0.61 °C, and 0.52 °C, respectively. Tang and Guo [25] examined the pavement temperature nowcasting experiments for the next 3 h at the Dongling Station on the Shenyang Third Ring Road (G1501) using the autoregressive summation moving average method with observations of the previous 23 h, exhibiting the mean absolute error of 0.26 °C. However, only 8 groups of experiments in 16 days are considered, and the forecast times mainly concentrate in the early morning, which might lead to some uncertainties of the results.

With respect to the current study with 12,384 sets of nowcasting experiments, the prediction results at Station V0001 (V0002) for lead times of every 10 min in 1 h show absolute errors of 0.17 °C (0.13 °C), 0.24 °C (0.20 °C), 0.35 °C (0.28 °C), 0.46 °C (0.36 °C), 0.57 °C (0.45 °C) and 0.68 °C (0.53 °C), respectively. Comparisons suggest that the pavement temperature nowcasting skills derived from the mean-generation function model in this study are generally equivalent to those of Wang et al. [26] using the random forest method. However, the experiment location of Xianyang Airport Expressway is characterized by a great complexity in the local environment, including the dense traffic flow and large amount of people as well as the heat island effect, making the corresponding nowcasting more difficult than the ordinary expressways. Moreover, the proposed nowcasting method provides the temporally refined results with the time interval being only 10 min in the present study.

Regarding the evaluations on forecast accuracy, the study follows the discrimination in Dong et al. [39] for intuitional comparisons of the forecast skills. They conducted a kind of qualitative categorized prediction on pavement temperatures using several statistical methods and revealed that the multivariate regression method is fairly effective in predicting the low pavement temperatures of <0 °C in northern Jiangsu with the forecast accuracies mostly being greater than 85%, while the support vector machine model is determined as the optimal for southern Jiangsu, and the corresponding accuracies reach almost 95%. By contrast, here in the current paper, the proposed nowcasting method for pavement temperatures using the mean-generation function model not only supplies effective and accurate nowcasting results for the decision makers, but also gives quantitative prediction results of pavement temperatures.

3.2.3. Nowcasting Skills Influenced by Weather Conditions and Initialization Time

To a great extent, the weather conditions have crucial impacts on not only the pavement temperature itself but also the corresponding nowcasting effect. Figure 7 displays the nowcasting evaluations of pavement temperatures under different weather conditions for the two stations. At the early stages, the forecast skills are generally similar with mean absolute errors being <0.2 °C for all the three conditions. When the lead time increases, the forecast errors increase significantly. The largest growing rates occur on sunny days, followed by the cloudy days, while the growing rates are slower on rainy and snowy days, which might be associated with the relatively small variability of pavement temperatures on rainy and snowy days. As the effect of the direct solar heating on the thermal sensors is not considered, the measurement error of pavement temperature on sunny days may

increase. This might also be one reason for the lower accuracy of pavement temperature forecast on sunny days.

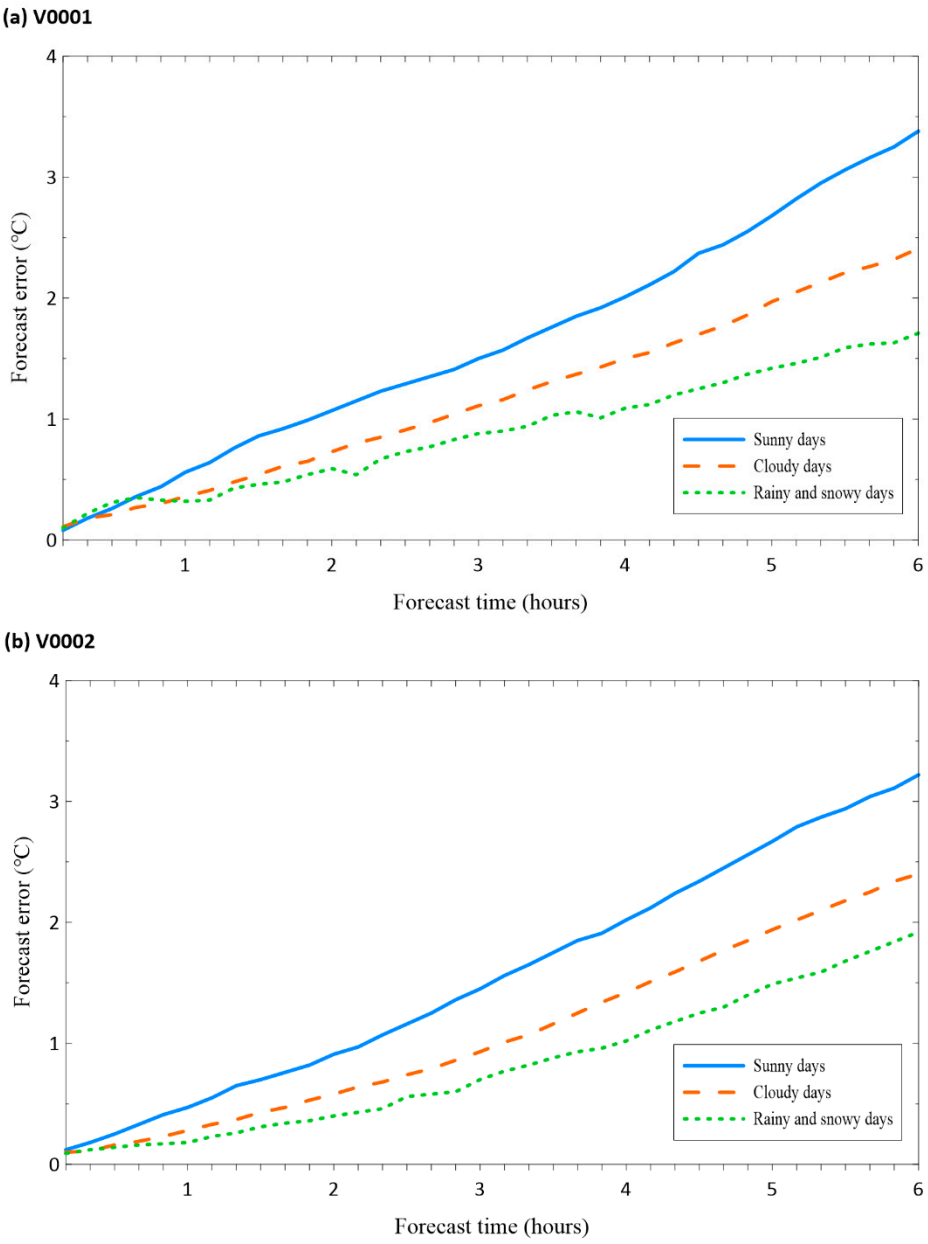

Figure 7. Errors of the pavement temperature nowcasting experiments under different weather conditions for Stations V0001 (**a**) and V0002 (**b**), respectively.

Meanwhile, prediction results in Wang et al. [26] based on the random forest regression method also indicate the highest forecast skills of pavement temperatures on rainy and snowy days, followed by cloudy days, and the worst on sunny days. When the pavement is covered by snow, or ice, etc., the heat exchanges between the ground and the atmosphere become weak or even disappears. The pavement temperature is rarely influenced by external factors and is relatively stable [2,31]. Such a phenomenon is also demonstrated by analyses on the transportation meteorological observations on roads and bridges [40,41].

Due to the significant diurnal variation characteristics of the pavement temperature, the nowcasting skills differ obviously among experiments initialized at different times (Figure 8). The mean absolute errors at the lead times of 1 h and 2 h for the two stations both show generally larger (smaller) values when initialized in the daytime (nighttime).

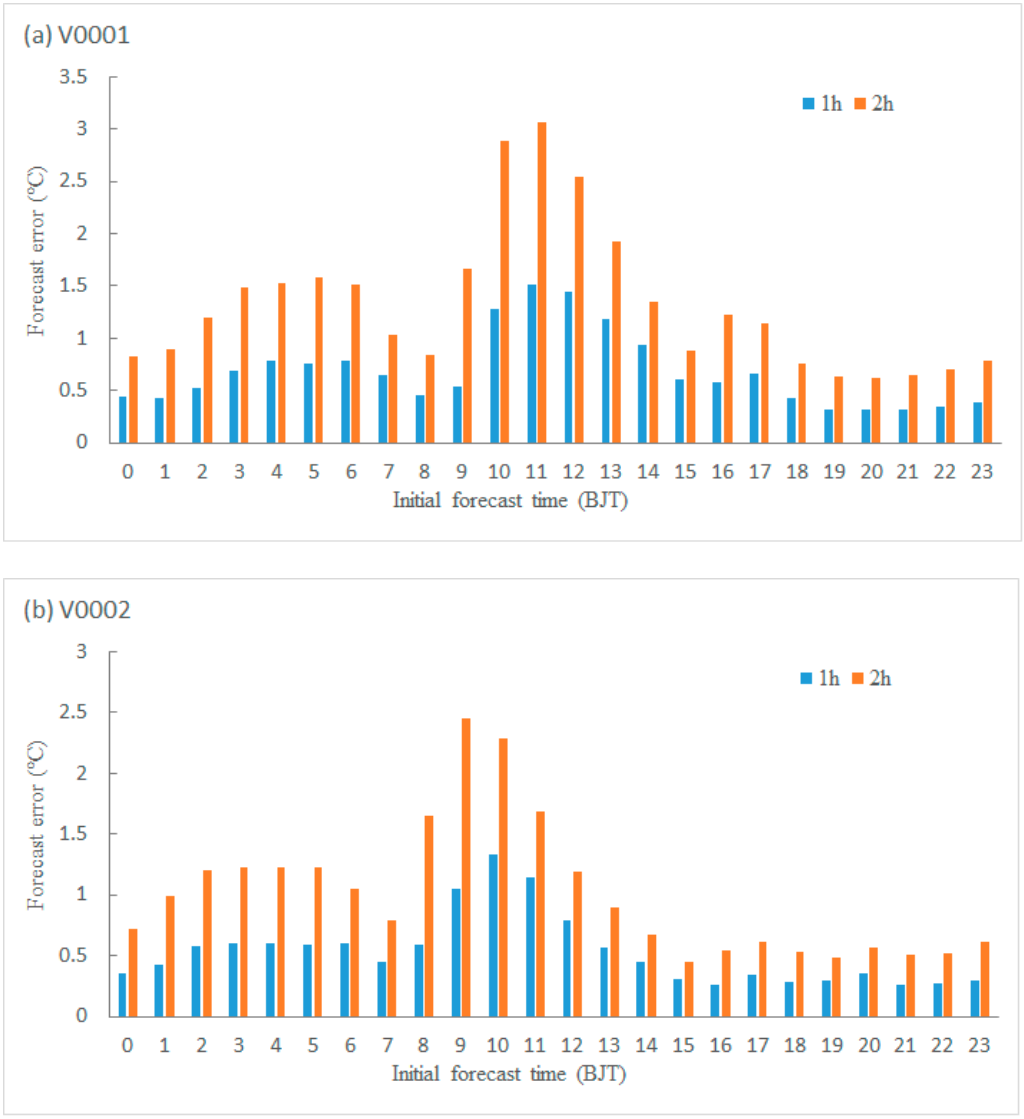

Figure 8. Errors of the pavement temperature nowcasting experiments initialized at different times for Stations V0001 (**a**) and V0002 (**b**), respectively.

For Station V0001, the absolute errors of the pavement temperature nowcasting initialized at the daytime (nighttime) at the lead time of 1 h range between 0.4 °C and 1.5 °C (0.3 °C and 0.7 °C), while they are distributed between 0.2 °C and 1.3 °C (0.2 °C and 0.6 °C) for Station V0002. The plot also suggests that the nowcasting errors of pavement temperature rise rapidly with the increase in lead times. At the lead time of 2 h, the nowcasting experiments initialized at daytime and nighttime show absolute errors of 0.8–3.0 °C and 0.6–1.5 °C, respectively, for Station V0001, while 0.4–2.4 °C and 0.4–1.2 °C for Station V0002.

3.2.4. Nowcasting Experiments at Different Regions

Aiming at exploring the applicability of the proposed method in different regions, similar nowcasting experiments on pavement temperature have been carried out towards the typical transportation meteorological stations in Beijing, Hubei and Tibet for the winter of 2021/2022. The nowcasting skills are compared with Station V0002, which are all displayed in Figure 9.

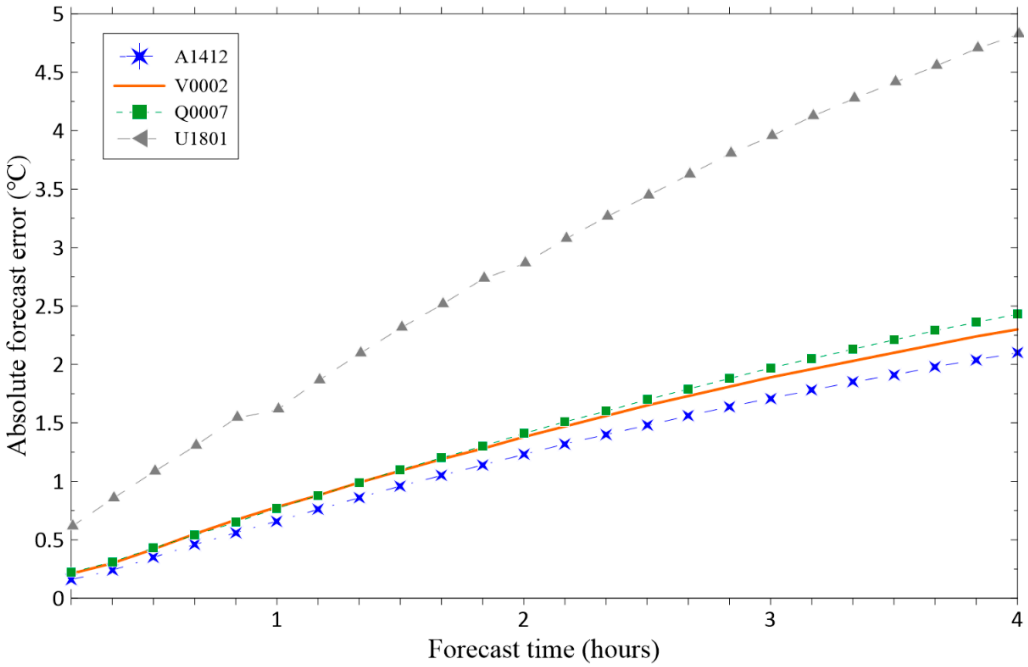

Figure 9. Errors of the pavement temperature nowcasting experiments at different stations in multiple areas.

The results show that the three stations in plain areas with lower altitudes (75 m, 41 m, and 708 m for Stations A1412, V0002, and Q0007, respectively) do not show much difference in the nowcasting errors within lead times of 4 h. Among them, Station A1412 in Beijing is characterized by the highest skills of pavement temperature nowcasting, with the absolute errors being 0.6 °C, 1.2 °C, 1.7 °C, and 2.1 °C for lead times of 1 h, 2 h, 3 h, and 4 h, respectively. However, the nowcasting errors of pavement temperature at Station U1801 in Tibet with the altitude of 3610 m display significantly larger values than the abovementioned three, which have already reached 1.6 °C at the lead time of 1 h. On the other hand, in terms of the ratios between the mean square deviations of the forecast errors and those of the observed pavement temperature series, the values are relatively small for Station U1801, i.e., 0.16, 0.25, and 0.34 at lead times of 1 h, 2 h and 3 h, respectively. It implies that although the pavement temperatures over the plateau area with complex terrain are generally more difficult to be predicted due to their larger variabilities, the proposed nowcasting method using the mean-generation function model in this study has certain reference values for the practical businesses of local early warnings and predictions of the low pavement temperature.

4. Conclusions

Using the pavement temperature observation data of the two transportation meteorological stations along the Xianyang Airport Expressway in Shanxi, China, as well as the datasets of precipitation and sunshine hours obtained from the nearby weather stations, the variation characteristics of local pavement temperatures were investigated for winter in this study. On this basis, a nowcasting method was proposed using a regression model via extracting the corresponding periodic features. Nowcasting experiments were then conducted and analyzed on the local pavement temperatures for the next 6 h with a rolling frequency of 10 min and a time interval of 10 min. The conclusions could be summarized as follows:

(1) Regardless of the weather condition, the observed temperature series are always characterized by significant diurnal variation characteristics, with the highest and lowest values occurring at around 14:00 and 07:00, respectively. Among the different weather conditions, during the daytime, the pavement temperature is the highest on sunny days,

followed by the cloudy days, with those on rainy and snowy days being the lowest. As for the nighttime, it shows highest pavement temperatures on non-icing rainy and snowy days, followed by the cloudy days, and the temperatures on sunny days are further lower, with those on icing rainy and snowy days being the lowest.

(2) The pavement temperatures at the Xianyang Airport Expressway are revealed with not only a significant 24 h periodic oscillation, but also high-frequency oscillation characteristics of about 12 h, 8 h, 6 h, 5 h and 4 h. The nowcasting based on the extraction of these periodic features using the mean-generation function model are demonstrated with considerable skills on predicting the local pavement temperatures. Examinations show the mean absolute errors of 0.2 °C, 0.6 °C, 1.2 °C and 1.5 °C for lead times of 20 min, 1 h, 2 h and 3 h, respectively.

(3) Comparisons among the pavement temperature nowcasting under different weather conditions indicate that the errors are smallest on rainy and snowy days, followed by cloudy days, and the skills are lowest on sunny days. This could be attributed to the more complex influence processes from factors such as clouds and radiation during the sunny days, as well as the larger variability of pavement temperatures. Furthermore, it also shows different nowcasting skills for different initialization times. The errors are generally higher (lower) for nowcasting experiments initialized in the daytime (nighttime), with the mean absolute errors of 0.7 °C and 1.4 °C (0.4 °C and 0.9 °C) for lead times of 1 h and 2 h, respectively.

(4) The expanded experiments for multiple transportation meteorological observation stations in Beijing, Hubei and Tibet demonstrate considerable universality and applicability of the method on pavement temperature nowcasting. It could achieve skillful nowcasting results in plain areas with lower altitudes but shows relatively insufficient performances in plateau areas with complex terrain. Nevertheless, considering the generally lower ratios between the mean square deviations of the forecast errors and those of the observed pavement temperature series, the nowcasting strategy can provide certain reference values for the practical businesses of local early warnings and predictions of the low pavement temperature.

5. Discussion

Changes in weather will affect the accuracy of the nowcast model. Two precipitation processes were picked to analyze the impact of weather change on the forecast skills. The results indicated that if the weather changes during the night, the impact on the forecast skill is smaller. However, if the weather changes during the day, the impact is larger, especially for the first several hours of weather change. With the rolling update of the nowcast model, the forecast results become closer to the observation, whereas the results need to be verified by more tests.

The statistical modeling method based on the extrapolation of high-frequency observations in pavement temperatures is demonstrated to be effective in the accurate nowcasting of pavement temperatures, which could provide an important basis for the identification of icing and snow covers on the pavement. In the road maintenance business, the advantages of an increase in accuracy of nowcasting products and a longer lead time of short-range forecast products are usually combined to arrange the road snow and ice removal. The prediction errors grow rapidly with the increase in lead times. Therefore, more detailed diagnoses and analyses on nowcasting errors are to be carried out in the future and would be favorable for more skillful nowcasting on the pavement temperatures [42,43]. Moreover, the statistical models could also be combined with the physical and dynamic models in the future [44,45].

Author Contributions: Methodology, L.F.; validation, L.F. and H.T.; data curation, M.L.; writing—original draft preparation, L.F. and L.M.; writing—review and editing, X.Y.; visualization, L.M.; project administration, H.T. All authors have read and agreed to the published version of the manuscript.

Funding: This research was funded by the National Key Research and Development program of China (Grant number 2020YFB1600103), the FengYun Application Pioneering Project (Grant number FY-APP-2021.0111) and the Innovation Fund Project of Public Meteorological Service Center of China Meteorological Administration (Grant number K2021006).

Institutional Review Board Statement: Not applicable.

Informed Consent Statement: Not applicable.

Data Availability Statement: The used data in this study are obtained from the data platform of China Meteorological Administration.

Conflicts of Interest: The authors declare no conflict of interest.

References

1. Brodsky, H.; Hakkert, A.S. Risk of a road accident in rainy weather. *Accid. Anal. Prev.* **1988**, *20*, 161–176. [CrossRef]
2. Sun, J.; Liang, F.; Chen, M.; Liao, X. An Analysis on Serious City Traffic Trouble Caused by Light Snow. *Chin. J. Atmos. Sci.* **2003**, *27*, 1057–1066.
3. Jiang, J.; Shi, L.; Ni, Y. A simulation of a high impact weather event. *J. Appl. Meteor. Sci.* **2005**, *16*, 231–237.
4. Zhu, S.; Yang, H.; Liu, D.; Wang, H.; Zhou, L.; Zhu, C.; Zu, F.; Wu, H.; Lyu, Y.; Xia, Y.; et al. Observations and Forecasts of Urban Transportation Meteorology in China: A Review. *Atmosphere* **2022**, *13*, 1823. [CrossRef]
5. Rayer, P.J. The Meteorological Office Road Surface Temperature Model. *Meteorol. Mag.* **1987**, *116*, 180–191.
6. Sass, B.H. A Numerical Model for Prediction of Road Temperature and Ice. *J. Appl. Meteorol.* **1992**, *31*, 1499–1506. [CrossRef]
7. Sass, B.H. A Numerical forecasting system for the prediction of slippery roads. *J. Appl. Meteorol.* **1997**, *36*, 801–817. [CrossRef]
8. Shao, J.; Lister, P. An Automated Nowcasting Model of Road Surface Temperature and State for Winter Road Maintenance. *J. Appl. Meteorol.* **1996**, *35*, 1352–1361. [CrossRef]
9. Crevier, L.P.; Delage, Y. METRo: A New Model for Road-Condition Forecasting in Canada. *J. Appl. Meteorol.* **2001**, *40*, 2026–2037. [CrossRef]
10. Shao, J.; Lister, P. The Prediction of Road Surface State and Simulation of the Shading Effect. *Bound.-Layer Meteorol.* **1995**, *73*, 411–419. [CrossRef]
11. Chapman, L.; Thornes, J. The influence of traffic on road surface temperatures: Implications for thermal mapping studies. *Meteor. Appl.* **2005**, *12*, 371–380. [CrossRef]
12. Bouilloud, L.; Martin, E.; Habets, F.; Boone, A.; Le Moigne, P.; Livet, J.; Marchetti, M.; Foidart, A.; Franchisteguy, L.; Morel, S.; et al. Road surface condition forecasting in France. *J. Appl. Meteorol. Climatol.* **2009**, *48*, 2513–2527. [CrossRef]
13. Kann, A.; Kršmanc, R.; Habrovský, R.; Šajn Slak, A.; Bujňák, R.; Schmid, F.; Tarjáni, V.; Wang, Y.; Wastl, C.; Bica, B.; et al. High-resolution nowcasting and its application in road maintenance: Experiences from the INCA central European area project. *IET Intell. Transp. Syst.* **2015**, *9*, 539–546. [CrossRef]
14. Feng, L.; Wang, X.; He, X.; Gao, J. Fine forecast of high road temperature along Jiangsu highways based on INCA system and METRo model. *J. Appl. Meteor. Sci.* **2017**, *28*, 109–118.
15. Liu, X.; Yu, Y.; Lei, G.; Liu, Z. Using radiant balance theory to calculate concrete road-surface temperature in summer. *J. Appl. Meteor. Sci.* **2004**, *15*, 623–628.
16. Zhu, C.; Xie, Z.; Yang, M.; Jing, Y. Study on numerical prediction model of extreme temperature on speedway-surface. *J. Meteorol. Sci.* **2009**, *29*, 645–650.
17. Tian, H.; Wu, H.; Zhao, L.; Chen, H.; Li, K.; Yang, X. Characteristics and statistical model of road surface temperature on Huning expressway. *J. Appl. Meteor. Sci.* **2009**, *20*, 737–744.
18. Niu, S.; Li, R.; Lyu, J.; Meng, L.; Ke, Y.; Yang, Z.; Xiong, S. Research on a numerical model for predicting three types of underlying surface temperature and ice. *Chin. J. Geophys.* **2011**, *54*, 909–917.
19. Meng, C.; Zhang, C. Development and verification of a numerical forecast model for road meteorological services. *J. Appl. Meteor. Sci.* **2012**, *23*, 451–458.
20. Feng, T.; Li, X.; Ding, D. Prediction of expressway surface temperature. *J. Highw. Transp. Res. Dev.* **2012**, *29*, 19–29.
21. Wu, H.; Ma, C.; Yang, R.; Zhang, J. Variation Characteristics of road surface temperature on highway of Hebei Province and its prediction model. *J. Arid Meteorol.* **2014**, *32*, 665–676.
22. Zhang, X.; Hao, Y.; Liang, J.; Pan, L.; Shen, J.; Lu, S. Characteristics of Road Surface Temperature of Shaanxi Expressway and Its Prediction Model. *J. Arid Meteorol.* **2019**, *37*, 1028–1034.
23. Wang, J.; Guo, C.; Gu, X. Study on Variation Characteristics and Prediction Model of Different Pavement Temperature in Baotou. *Desert Oasis Meteorol.* **2021**, *15*, 91–96.
24. Lin, Z.; Hu, J.; Zhu, C. A Method for Forecasting Hourly Expressway Surface Temperature during Night Time. *J. Highw. Transp. Res. Dev.* **2021**, *38*, 23–29.
25. Tang, J.; Guo, Z. Pavement Temperature Short-impending Prediction Based on ARIMA in Winter. *J. Tongji Univ. (Nat. Sci.)* **2017**, *45*, 1824–1829.

26. Wang, K.; Bao, Y.; Zhu, C.; Chen, C.; Yuan, C. Forecasts of road surface temperature in winter based on random forests regression. *Meteorol. Mon.* **2021**, *47*, 82–93.
27. Qu, X.; Qi, Y.; You, Q.; Wang, Y.; Wu, D.; Li, M. An approaching prediction method of road surface temperature of Winter Olympic Highway demonstration station based on METRo model. *J. Arid Meteorol.* **2020**, *38*, 497–503.
28. Wu, S.; Wu, D.; Deng, X.; Tan, H. Characteristics of road surface temperature on freeway over Nanling Hilly region. *Meteorol. Sci. Technol.* **2006**, *34*, 783–787.
29. Ma, J.; Liao, C.; Zhang, Y. Variation Characteristics of Road Surface Temperature on Highway of Changsha and Its Prediction Model. *Sci. Mosaic* **2017**, *2*, 22–25.
30. Bao, G.; Wang, W.; Zhang, J.; Zhang, J.; Ma, S.; Pei, S. Temporal-spatial distribution of road icing in Qinghai and its impact. *Meteorol. Sci. Technol.* **2016**, *44*, 104–110.
31. Zhang, H.; Lu, S.; Shen, J.; Zhang, X.; Dang, C. Temporal and Spatial Distribution Characteristics of Road Icing in Shaanxi and Its Risk Warning Model. *J. Arid Meteorol.* **2020**, *38*, 878–885.
32. Wei, F. *Modern Climate Statistical Diagnosis and Prediction Technology*; China Meteorological Press: Beijing, China, 2005; pp. 71–75.
33. Bai, Y.; Gao, X.; Zhang, W.; Xi, C.; Wang, L. Analysis of the array data power spectrum in Hailar. *Seismol. Res. Northeast China* **2020**, *36*, 49–55.
34. Feng, L.; Wei, F.; Zhu, Y. A predictive model for summer precipitation over China based on upper tropospheric temperature and North Atlantic Oscillation in the preceding spring. *Chin. J. Atmos. Sci.* **2011**, *35*, 963–976.
35. Wei, F.; Han, X.; Wang, Y.; Chen, G. *Physical Basis of Short-Term Climate Prediction in China and Short-Term Climate Prediction Methods*; China Meteorological Press: Beijing, China, 2015; pp. 211–222.
36. Chang, R.; Zhu, R.; Liu, Y.; He, X. Nowcasting model of wind speed based on mean generating function for wind farms. *Meteorol. Mon.* **2013**, *39*, 226–233.
37. Sun, Q.; Li, J.; Hu, T.; Han, W. Study on variation of road surface temperature. *J. China Foreign. Highw.* **2015**, *35*, 32–36.
38. Zhang, C.; Tan, Q.; Tang, S.; Gao, X. Classification and combination prediction model for wind power based on change period of wind speed. *Acta Energ. Sol. Sin.* **2017**, *4*, 999–1006.
39. Dong, T.; Bao, Y.; Yuan, C.; Zhou, L.; Jiao, S. Application of Three Statistical Forecast Models in Early Warning of Low Tem-perature on Road Surface in Jiangsu and Their Comparison. *Meteorol. Sci. Technol.* **2018**, *46*, 773–784.
40. Lyu, J.; Niu, S.; Zhou, Y.; Li, R.; Ke, Y.; Yang, Z. Characteristic of bridge and road surface temperature changes in winter and energy budget analysis. *Trans. Atmos. Sci.* **2013**, *36*, 546–553.
41. Wang, J.; Zhu, C.; Yuan, C.; Bao, Y. Study of low temperature differences between road surface and bridge surface on Yang-zhou-Liyang expressway in winter. *J. Trop. Meteorol.* **2018**, *34*, 279–288.
42. Lyu, Y.; Zhi, X.; Wu, H.; Zhou, H.; Kong, D.; Zhu, S.; Zhang, Y.; Hao, C. Analyses on the Multimodel Wind Forecasts and Error Decompositions over North China. *Atmosphere* **2022**, *13*, 1652. [CrossRef]
43. Fan, Y.; Zhu, S.; Wang, L.; Wang, X. Subseasonal dynamical prediction of South China Sea summer monsoon. *Atmos. Res.* **2022**, *278*, 106347. [CrossRef]
44. Zhu, S.; Zhi, X.; Ge, F.; Fan, Y.; Zhang, L.; Gao, J. Subseasonal forecast of surface air temperature using superensemble ap-proaches: Experiments over Northeast Asia for 2018. *Weather Forecast* **2021**, *36*, 39–51. [CrossRef]
45. Lyu, Y.; Zhi, X.; Zhu, S.; Fan, Y.; Pan, M. Statistical calibrations of surface air temperature forecasts over East Asia using pattern projection methods. *Weather Forecast* **2021**, *36*, 1661–1674. [CrossRef]